Princeton Plasma Physics Laboratory

PPPL- 4687

PPPL- 4687

Electromagnetic and Structural Analysis of ITER Central Solenoid Insert Coil

Andrei E. Khodak, Nicolai N. Martovetsky,
Alexandre V. Smirnov, and Peter H. Titus

September, 2011

PPPL PRINCETON PLASMA PHYSICS LABORATORY

Prepared for the U.S. Department of Energy under Contract DE-AC02-09CH11466.

Princeton Plasma Physics Laboratory
Report Disclaimers

Full Legal Disclaimer

Trademark Disclaimer

PPPL Report Availability

Princeton Plasma Physics Laboratory:

http://www.pppl.gov/techreports.cfm

Office of Scientific and Technical Information (OSTI):

http://www.osti.gov/bridge

Related Links:

U.S. Department of Energy

Office of Scientific and Technical Information

Fusion Links

Electromagnetic and Structural Analysis of ITER Central Solenoid Insert Coil

Andrei E. Khodak, Nicolai N. Martovetsky, Alexandre V. Smirnov, Peter H. Titus

***Abstract*—The United States ITER Project Office (USIPO) is responsible for fabrication of the Central Solenoid (CS) for International Thermonuclear Experimental Reactor (ITER). The CS Insert (CSI) project should provide verification of the conductor performance in relevant conditions of temperature, field, currents and mechanical strain. The USIPO will build the CSI that will be tested at the Central Solenoid Model Coil (CSMC) Test Facility at JAEA, Naka, Japan. This paper presents three-dimensional mathematical model of CSI based on the design. Simulations were performed in order to verify structural integrity and compliance with the Japanese High Gas Pressure Safety Law. Numerical simulations lead to the design of the CSI that produced a required strain levels during operation on the superconductor cable, while simultaneously satisfy the ITER magnet structural design criteria.**

***Index Terms*— Superconducting magnets, Numerical analysis, Computational modeling, Finite element methods**

I. INTRODUCTION

THE CSI assembly is presented on Fig. 1. It consists of a one layer superconducting coil with 8.75 turns. This coil is placed between the spacers into a support structure. The support structure provides pre-compression of the coil using tie-rods, and also positioning of the coil within the CSMC structure by way of four mounting bolts at the bottom flange, and four mounting jacks on the top flange. Electric current is supplied to the superconducting coil by bus bars connected to the coil leads trough lap joints. The CSI is designed to test the conductor, in the magnetic field generated by CSMC. Design and performance of CSMC are presented in [1].

Manuscript received 12 September 2011. This manuscript has been authored by PPPL under contract DE-AC02-09CH11466 and UT-Battelle, LLC under contract DE-AC05-00OR22725 with the U.S. Department of Energy. All US activities are managed by the US ITER Project Office, hosted by Oak Ridge National Laboratory with partner labs Princeton Plasma Physics Laboratory (PPPL) and Savannah River National Laboratory. The project is being accomplished through a collaboration of DOE Laboratories, Universities and industry. The United States Government retains and the publisher, by accepting the article for publication, acknowledges that the United States Government retains a non-exclusive, paid-up, irrevocable, world-wide license to publish or reproduce the published form of this manuscript, or allow others to do so, for the United States Government purposes.

A. E. Khodak and P. H. Titus are with the Princeton Plasma Physics Laboratory, Princeton, NJ 08543 USA phone: 609-243-3028; fax: 609-243-3030; e-mail: akhodak@pppl.gov.

N. N. Martovetsky and A. V. Smirnov are with the Oak Ridge National Laboratory, Oak Ridge, TN 37831 USA.

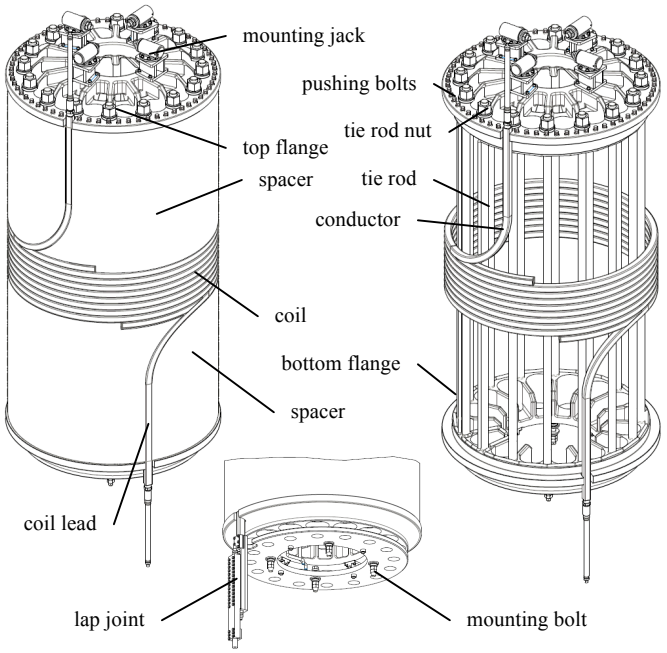

Fig. 1. CSI assembly on the left: assembly with wraparound insulation removed; on the right: spacers are also removed to show support structure. Mounting details and lap joint are shown at the bottom

We used finite element analysis (FEA) based on ANSYS software [2] to verify and optimize performance of the CSI design. Three-dimensional (3D) nature of the design, required development of 3D numerical model capable of predicting effects of the asymmetrical electromagnetic loading since the coil does not have whole number of windings. 3D numerical simulations were performed using coupled solver for simultaneous structural, thermal, and electromagnetic analysis. Thermal and electromagnetic simulations supported structural calculations providing necessary loads and strains. Simulations were performed during design process to verify structural integrity. Several modifications of the initial design were made to improve performance under load conditions.

II. NUMERICAL MODEL

A. Geometry and Meshing

The CSI insert model geometry was created using computer aided design (CAD). To allow efficient meshing geometry of the model was split into blocks that can be swept, within ANSYS Workbench [2]. Splitting of the model into blocks does not introduce any additional geometrical simplifications and was used to allow 3D hexahedra meshing. Meshing was performed within the standalone version of ANSYS.

B. Boundary Conditions and Loads

The model is fixed in the axial and tangential directions at four rods representing mounting bolts at the bottom. The other four rods at the bottom are restricted only in tangential direction, representing sliding in the rails. At the top, the CSI is restricted in radial direction by support boots. Preload of the support boots is simulated using cylindrical volumes with elastic modulus adjusted to achieve designed spring force of 35.75 kN at 7 mm initial displacement.

Constant temperature at all nodes was imposed on the model at each solution step. Room temperature results were obtained at 293K. The temperature of 4K represented condition after cool down.

Pre-tension of 100MPa at 293K is introduced in rods using special elements, which convert pretension into displacement at the first step. Pre-compression of 25MPa was introduced in the lap joint in a similar manner. Internal helium pressure load of 3MPa was imposed on internal surface of the jacket and sleeve. Sliding interfaces were created to simulate effect of Teflon inserts between the jacket and the spacers, and spherical washers at the tie-rod ends.

Electrical boundary conditions were imposed on the opposing ends of the superconductor cable, to simulate constant current flow of 0 or 60kA.

The external magnetic field is simulated using current conducting source elements, representing geometry and charge of the CSMC windings, and creating 13T vertical magnetic field in the area of CSI coil.

A. Material Properties

Material properties used are summarized in Table 1.

TABLE 1 Material Properties

Part	Material	Elastic Modulus [GPa]		0.2% Yield Stress [MPa]		Thermal Strain
		293 K	4 K	293K	4K	4 K
Flanges Spacers	AISI316L	192	207	170	800	-0.27%
Spacers	Titanium	116	116	140	300	-0.15%
Jacket	JK2LB	192	200	200	700	-0.197%
Tie-Rods	Aluminum Al7075-T6	69	82	450	530	-0.38%
Super-conductor Cable	Smeared Properties	along cable: 20 across cable: 1.5				-0.197%
Insulation	Composite	in plane: 20 across plane: 12				-0.25% -0.7%
Pushing Bolts	Inconel-718	200	216	1100	1350	-0.315%
Connector	Copper CDA102	117	117	MKIN model		-0.27%

Isotropic elastic structural model with temperature dependent properties was used for all materials with the exception of orthotropic model for insulation and superconductor material and elastic-plastic model for copper conductor in the lap joint.

Since thermal contraction of aluminum tie-rods at 4K is larger than that of the spacers and the cable, additional pretension is achieved in the CSI assembly after cool down. This effect allows imposing a lower initial pretension at room temperature, when the yield stress of the materials are lower, and gain full strength of targeted pretension at 4K when yield stresses are much higher as shown in Table 1.

Properties of superconductor cable are considered smeared. Elastic modulus for the smeared module in accordance with [3] is assumed 20GPa along the cable and 1GPa across with zero Poisson's ratio.

III. Current Sharing Temperature Distribution

One of the problems of the CSI is to assure that the properties of the conductor near the median plane are measured accurately. Since Nb3Sn is strain sensitive and electromagnetic forces generate a significant strain that increase the current sharing temperature (Tcs), there is a dilemma. We need to design the Insert in such a way that the mostly strained conductor near the median plane would still have the lowest Tcs than the rest of the conductor in the Insert, particularly the conductor that is adjacent to the spacers. Otherwise, our ability to measure performance of the conductor will be limited, since the lowest Tcs will be in the conductor near the spacers, not in the median plane. Since the magnetic field is pretty uniform, we have to do some strain management to the turns that are adjacent to the spacers. Our first material choice of the spacer was stainless steel. The problem of lower Tcs outside of the median plane turns was severe and titanium spacer was studied, as described below.

Distribution of the Tcs was obtained from numerical results using parameterization of the critical surface in the form similar to proposed for ITER in [4]:

$$I_C = \frac{C_1}{B} s(\varepsilon)\left(1-\left(\frac{T}{T_C^*}\right)^{1.52}\right)\left(1-\left(\frac{T}{T_C^*}\right)^{2}\right)\left(\frac{B}{B_{C2}^*}\right)^{p}\left(1-\left(\frac{B}{B_{C2}^*}\right)\right)^{q} \quad (3)$$

$$B_{C2}^*(T,\varepsilon) = B_{C20\max}^* s(\varepsilon)\left(1-\left(\frac{T}{T_C^*}\right)^{1.52}\right) \quad (4)$$

$$T_C^*(B,\varepsilon) = T_{C0\max}^*\left[s(\varepsilon)\right]^{1/3} \quad (5)$$

$$s(\varepsilon) = 1 + \frac{C_{a1}\left(\sqrt{\varepsilon_{sh}^2+\varepsilon_{0,a}^2} - \sqrt{(\varepsilon-\varepsilon_{sh})^2+\varepsilon_{0,a}^2}\right) - C_{a2}\varepsilon}{1-C_{a1}\varepsilon_{0,a}} \quad (6)$$

$$\varepsilon_{sh} = C_{a2}\varepsilon_{0,a} \Big/ \sqrt{C_{a1}^2 - C_{a2}^2} \quad (7)$$

where:

I_C – critical current [A] that generates electrical field of 10 microVolts/m

ε – strain along the cable

B – combined magnetic field intensity [T]

Equations (3)-(7) characterize superconductor strand in the cable with the current direction perpendicular to the magnetic field. In the areas where coil and field directions are not perpendicular, we include a special correction based on experimental results summarized in [5]. This correction modifies scaling constant C_1 into a following function:

$$C_1(\beta) = C_1(90^\circ) \Big/ 0.62\cdot\sin\beta + 0.38 \quad (8)$$

where:

β – angle between current direction and magnetic field

$C_1(90°)$ – value of C_1 from Table 4

For known distributions of the longitudinal strain ε and magnetic field B the Tcs can be obtained resolving equations (3)-(8) for T with the constant value of I_C obtained as current through the conductor divided by the number of strands

$$I_c = I_t / N_s \tag{9}$$

where:

I_t – total transport current through conductor

N_s – number of superconducting strands (576)

The characterization of the $I_C(\varepsilon, T, B)$ was used with the parameters reported in [6] and presented in Table 2.

TABLE 2 Superconductor Characterization Parameters

Parameter	Value	Description
C_1	46636.	scaling constant
C_{a1}	44.16	strain fitting constant
C_{a2}	6.742	strain fitting constant
$\varepsilon_{0,a}$	0.002804	residual strain component
$B^*_{C20\max}$	31.75T	maximum critical field
$T^*_{C0\max}$	16.23K	maximum critical temperature
p	0.9419	low field exponent for pinning force
q	2.539	high field exponent for pinning force

IV. Simulation Results

Table 3 summarizes some of the results of the structural analysis as compared to design criteria from [7]. Results of peak stresses for the jacket are presented. All components of the CSI satisfied design criteria from [7].

TABLE 3 Structural Analysis Data

Temperature	Current	Peak Stress from Numerical Analysis	Peak Stress criteria
293K	0A	109MPa	200MPa
4K	0A	317MPa	700MPa
4K	direct 60kA	613MPa	700MPa
4K	reverse 60kA	384MPa	700MPa

A. Operating temperature of 4K with no current

During cool down to 4K the insert coil shrinks due to thermal contraction. Since the jacket is made of JK2LB steel it contracts less than the stainless steel spacers creating convex deformation shape as shown on the left side of Fig. 2. Titanium spacers contract less than JK2LB, so the deformation shape becomes convex on the right side of Fig. 2.

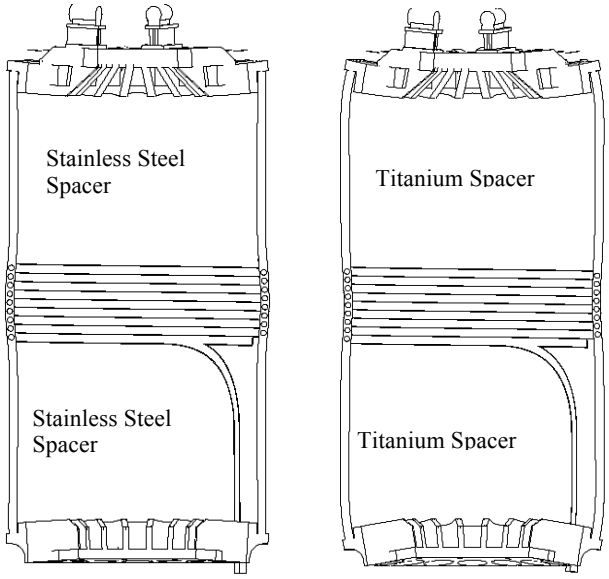

Fig. 2. CSI assembly cross-section after cool down to 4K. Deformation scale 40:1. Tie rods are not shown

Numerical simulations show additional pretension of 108 MPa due to difference in thermal contraction when stainless steel spacers are used. In the case of titanium spacers, additional pretension increases to 152MPa, resulting in higher deformation of the flanges as shown on Fig. 2.

B. Operating temperature of 4K direct charge 60 kA

We call "direct charge" the situation when magnetic field generated by the CSMC and CSI have the same sign on the axis as opposed to the "reverse charge". At the direct charge with 60 kA, the CSI bends in the direction opposing the incomplete portion of the windings due to the action of the Lorentz force. This force also expands the windings of the coil leading to convex deformation in the case of stainless steel spacers as shown on Fig. 3.

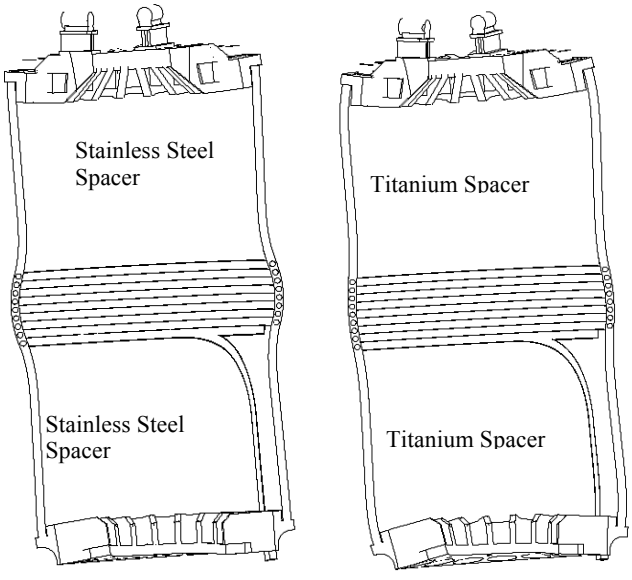

Fig. 3. CSI assembly cross-section at 4K. Direct charge 60kA. Deformation scale 40:1. Tie rods are not shown

In the case of titanium spacers, the deformation profile

switches from concave to convex when current is applied, however the convex shape is much less pronounced in this case, resulting in much more uniform strain distribution in the cable leading to more uniform distribution of the Tcs for titanium spacers as shown on Fig. 4.

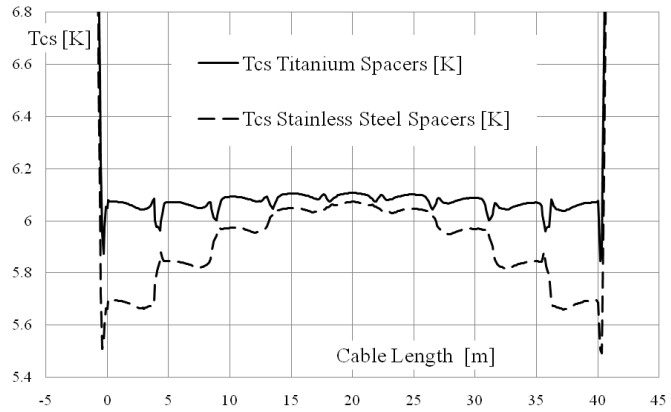

Fig. 4. Tcs distribution along the cable. Direct charge 60kA

Distributions in Fig. 4 were obtained using normal elastic strain values in the direction of the cable extracted from numerical simulation results. A uniform strain of –0.7% was added to include effect of differential thermal contraction of the jacket and the cable from the reaction temperature to 4K. -60kA current distributed on 576 strands was used in formula (9). Equations (3)-(8) were solved numerically at 0.1m intervals of the cable length. Distributions on Fig. 4 are shown relative to the length of the cable. Coil starts at zero position and extends 40 meters, the lead extension are at the extremes of this length. Results show that the current sharing temperatures vary no more than 0.2K in the region of the coil, and have higher values at the leads. The minima of current sharing temperature values are in the transition regions from coil to leads, but still allow measuring the Voltage-temperature characteristic to quench.

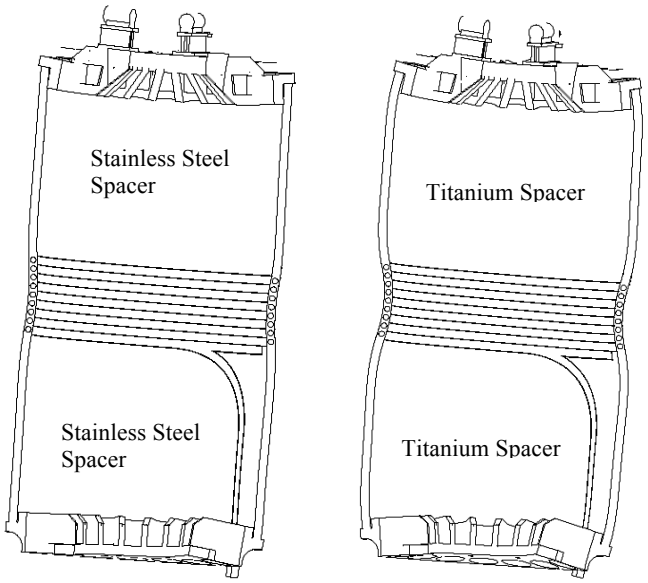

Fig. 5. CSI assembly cross-section at 4K. Reverse charge 60kA. Deformation scale 40:1. Tie rods are not shown

C. Operating temperature of 4K reverse charge 60 kA

When current is applied at 4K resulting in reverse charge of 60kA CSI bends in the direction of the incomplete portion of the windings due to the action of the Lorentz force. This force also contracts the windings of the coil leading to increased concave deformation as shown on Fig. 5.

In the case of titanium spacers the concave shape was achieved at 4K due to thermal contraction, and then augmented by the action of the Lorentz force. Thus the current sharing temperature profiles in Fig. 6 show more uniformity in the case of stainless steel spacers. This is still a desirable situation – when the Tcs is lower in the middle.

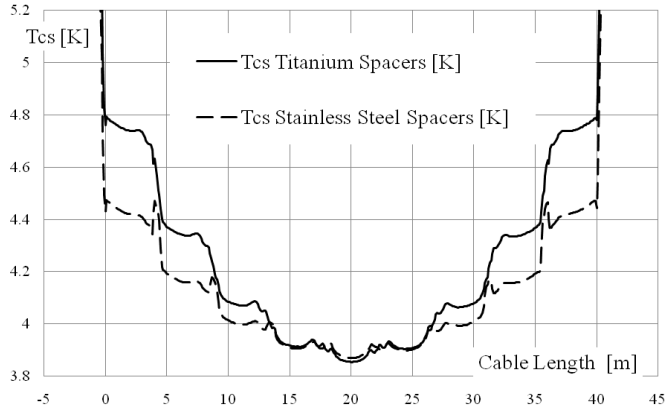

Fig. 6. Tcs distribution along the cable. Reverse charge 60kA

V. Conclusion

Numerical simulations of the CSI model were performed using ANSYS software allowing validation of the design. Three-dimensional computer modeling is necessary to optimize the design to satisfy ITER magnet structural design criteria in all operating regimes.

Numerical analysis of coil behavior provided confirmation for changing material to titanium for coil spacers. This change of the material increased Tcs in the transitional regions from coil to leads, so that Tcs values in the middle of the coil differ no more than 0.2K from the minimal values of Tcs in the entire cable. For original stainless steel spacers this difference is three times as large.

References

[1] N. Martovetsky, *et al.* "Test of the ITER Central Solenoid Model Coil and CS Insert," *IEEE Trans. on Applied Superconductivity*, vol. 12, no. 1, pp. 600–605, Mar. 2002.
[2] *ANSYS Workbench User's Guide,* ANSYS Inc., Canonsburg, PA, 2010.
[3] P. Titus, "Effective Longitudinal Modulus, and Jacket Tension," *Memo* 2007.
[4] L. Bottura, and B. Bordini, "$J_c(B,T,\varepsilon)$ Parameterization for the ITER Nb_3Sn Production," *IEEE Trans. on Applied Superconductivity*, vol. 19, no. 3, pp. 1521–1524, Jul. 2009.
[5] M. Takayasu, D.B. Montgomery, and J.V. Minervini, "Effect of Magnetic Field Direction on the Critical Current of Twisted Multifilamentary Superconducting Wires," *Advances in Cryogenic Engineering (Materials)*, vol. 44, 1998, pp. 1035–1042.
[6] Y. Nabara, JAEA, private communication.
[7] "Magnet Structural Design Criteria" ITER_D_2ES43Vv1.2

The views and opinions expressed herein do not necessarily reflect those of the ITER Organization

The Princeton Plasma Physics Laboratory is operated
by Princeton University under contract
with the U.S. Department of Energy.

Information Services
Princeton Plasma Physics Laboratory
P.O. Box 451
Princeton, NJ 08543

Phone: 609-243-2245
Fax: 609-243-2751
e-mail: pppl_info@pppl.gov
Internet Address: http://www.pppl.gov